PAPER H

3-D FINITE-DIFFERENCE ACOUSTIC WAVE EQUATION MODELING

Le-Wei Mo

SUMMARY

Forward modeling by construction of synthetic seismic data can be very useful in the interpretation of seismic time sections. In this kind of work, synthetic data are compared to field results to determine how the assumed geologic model of the subsurface needs to be modified to obtain better agreement between calculations and observations. Forward modeling is also very useful in suggesting how the field survey should be laid out in order to observe the response of the target. And forward modeling code can be readily turned into a reverse-time migration code.

In cross-well seismology, owing to the limitations of the availability of wells, the surveys are more likely to be carried out in two-dimensions. 3-D forward modeling can reveal whether a 2-D survey can adequately predict the geology in a province. One may simply argue that the earth is variant in 3-D. But depending on the relative magnitude of the seismic wavelength used in the survey and the dimensions of the geology targets, 3-D variant targets can be regarded as 2-D variant. An example is 2-D surface reflection seismology, this technology has been successfully used for many years.

In this paper, I address the problem of 3-D finite-difference acoustic wave equation modeling. 3-D wave equation modeling is an extremely computation intensive process, and it requires large computer memory. Here at STP, we do not have the supercomputer facilities to carry out large size 3-D computations. I describe how to use network connected workstations to share the computations and test the method on a small sized model. Additionally, I describe an effective and economical absorbing boundary condition and apply it for this 3-D modeling.

F-D EVALUATION OF THE WAVE EQUATION

Let us assume that the earth behaves like an acoustic medium in which the influence of variations in density can be safely ignored. In that case, the propagation of energy into the earth is governed by the acoustic wave equation

$$\left(\frac{\partial^2 U}{\partial^2 x}\right)+\left(\frac{\partial^2 U}{\partial^2 y}\right)+\left(\frac{\partial^2 U}{\partial^2 z}\right)=\frac{1}{v^2(x,y,z)}\left(\frac{\partial^2 U}{\partial^2 t}\right)+f(t)\delta(x-x_s,y-y_s,z-z_z) \qquad (1)$$

where $U(x,y,z)$ represents the wavefield and $v(x,y,z)$ denotes the velocity of the medium at spatial location (x,y,z), t denotes time, and $f(t)$ represents a time dependent band-limited source S located at (x_s,y_s,z_s).

In finite-differencing, I use i, j, k to represent the spatial coordinates x, y, z, and use n to represent the temporal coordinate t. I can write the wave field

$$U(x,y,z,t)=U^n_{i,j,k}, n=0,1,2,3,... \qquad (2)$$
$$f(t)=f_n$$

In solving the wave equation (1), I use tenth order finite-differencing to approximate the second order spatial derivatives, and use second order finite-differencing to approximate the second order temporal derivative (Dablain, 1986). In both the spatial and temporal derivatives, I use central finite-difference schemes because the wave equation is symmetic in both space and time.

$$\frac{\partial^2 U_i}{\partial^2 x}=\frac{1}{\Delta x^2}\left[w_0 U_i+\Sigma_{k=1}^{5} w_k\left(U_{i-k}+U_{i+k}\right)\right] \qquad (3)$$

$$\frac{\partial^2 U^n}{\partial^2 t}=\frac{U^{n+1}-2U^n+U^{n-1}}{\Delta t^2} \qquad (4)$$

The coefficients in the second order spatial derivative are calculated by an optimization method, which minimizes the dispersion for a given operator length of 11. The coefficients are w0 = -2.92722, w1 = 1.666667, w2 = -0.238095, w3 = 3.96825E-02, w4

= -4.96031E-03, and w5 = 3.17460E-04. In forward marching in time, I need to use three snap-shot wavefields: $U^1_{i,j,k}, U^2_{i,j,k}, U^3_{i,j,k}$. $U^1_{i,j,k}$ is the previous snap-shot wavefield, $U^2_{i,j,k}$ is the current snap-shot wavefield, these two wave fields are known. $U^3_{i,j,k}$ is the next time step wave field to be computed. The current wavefield $U^2_{i,j,k}$ is used to compute the spatial derivatives in equation (1) by finite-difference equation (3). The three spatial derivatives in equation (1) can be computed independently. In this case, I distributed the derivatives to be carried out in three separate DEC-Alpha workstations. The major requirement is that there be a common disk that could be accessed by several computers for data exchange. The master computer writes the wavefield $U^2_{i,j,k}$ to the common disk and sends a data-ready semaphore signal to the slave computers. The access to the shared data by the three slave computers is controlled by a semaphore. The slave computers compute the spatial derivatives in equation (3) and write the result to the shared disk and send a data-ready signal to the master computer. Finally, the derivatives are combined by the master computer to compute the unknown $U^3_{i,j,k}$ in equation (1).

ABSORBING BOUNDARY CONDITIONS

Appropriate implementation of absorbing boundary conditions is extremely important in 3-D wave equation modeling, because in 3-D, any extra grid padding at the boundary can rapidly increase the computer memory requirements and, consequently increase computation time. I found that an effective and economical absorbing boundary can be implemented by the following two steps. First, I apply the one-way wave equation

$$\frac{\partial U}{\partial t} + v\frac{\partial U}{\partial x} = 0 \tag{5}$$

to calculate $U^3_{i,j,k}$ at the boundary. Then I apply the following multiplication factor function:

$$G(i) = \exp\left(-\tfrac{h}{v} i^2\right) \tag{6}$$

where i is index distance from the actual useful grid boundary, h is the spatial sampling interval and v is the velocity at the boundary. At each time step, after $U^3_{i,j,k}$ is computed

by the above equation (4), the multiplication factor equation (6) is applied to both $U^2_{i,j,k}, U^3_{i,j,k}$.

$$U_i = U_i G(i), i = 0,...,8 \tag{7}$$

at the six boundary sides. Very good absorbing effect can be achieved by a padding width of 8, as compared to the suggested padding width of 20, by using a different multiplication factor (Cerjan, et al, 1985). Next, the wave field $U^2_{i,j,k}$ is copied into $U^1_{i,j,k}$, and $U^3_{i,j,k}$ is copied into $U^2_{i,j,k}$. The next time step is ready to start computation.

EXAMPLE

Figure 1 shows a 3-D velocity model with a 15-degree dipping interface separating two velocity strata, v1 = 14000 ft/s, v2 = 18000 ft/s. The discrete size of the model is 100x100x100. The x,y,z sampling intervals are 1.5 ft. The number of time steps is 1000. The time step is 0.2 ms. The second order derivative of the Gaussian function is used for the source (Alford et al, 1974). The computation time for one shot gather modeling is 2 hours and 10 minutes. In a cross-well survey, the receiver well is off the dip plane from the source. Figure 2 is a common shot gather. Figure 3 shows the first break travel times of direct arrival wave forms and the travel times calculalted by analytic ray tracing (Sheriff and Geldart, 1980, p81-85). They match pretty well. Figure 4 shows the amplitudes of the direct arrivals recorded in the upper layer against the theoretical *1/r* geometrical amplitude, where *r* is the propagation distance.

CONCLUSIONS

A 3-D finite-difference acoustic wave equation modeling code has been developed and tested on network connected workstations. The travel times of the wave forms are consistent with travel times obtained from analytic ray tracing. And the amplitude decays correctly as in analytic results. The new absorbing boundary condition introduced in this paper is shown to be effective, and it requires less than half of the boundary padding that existing methods require. The new absorbing boundary condition can find good applications, especially in the 3-D computation. The network parallel computations make 3-D wave equation computations feasible at our group at the present time. This modeling code can be readily transformed into a reverse-time migrartion code.

REFERENCES

Alford, R. M., Kelly, K. R., and Boore, D. M., 1974, Accuracy of finite-difference modeling of the acoustic wave equation: Geophysics, 39, 834-842.

Dablain, M. A., 1986, The application of high-order differencing to the scalar wave equation: Geophysics, 50, 870 - 880.

Cerjan, C., Kosloff, D., and Reshef, M., 1985, A nonreflecting boundary condition for discrete acoustic and elastic wave equations.: Geophysics, 51, 1650 - 1655.

Sheriff, R. E., and Geldart, L. P., 1980, Exploration Seismology: Vol. 1, Cambridge University Press.

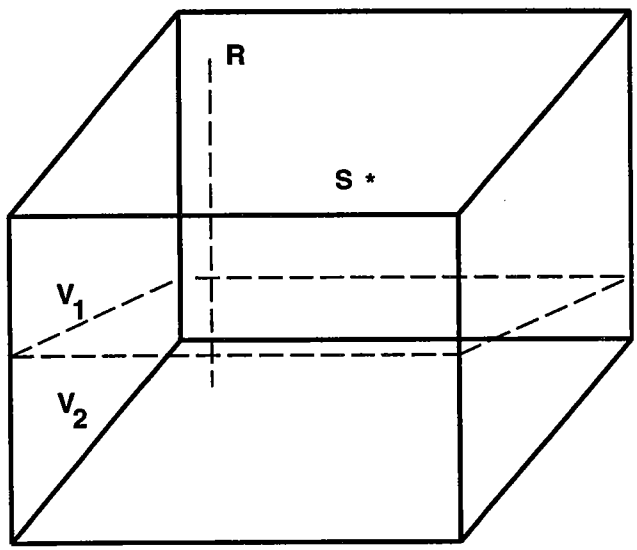

Figure 1. A 3-D velocity model with a dipping interface. S is the source, R is the receiver well. The receiver well is off the dip plane from the source.

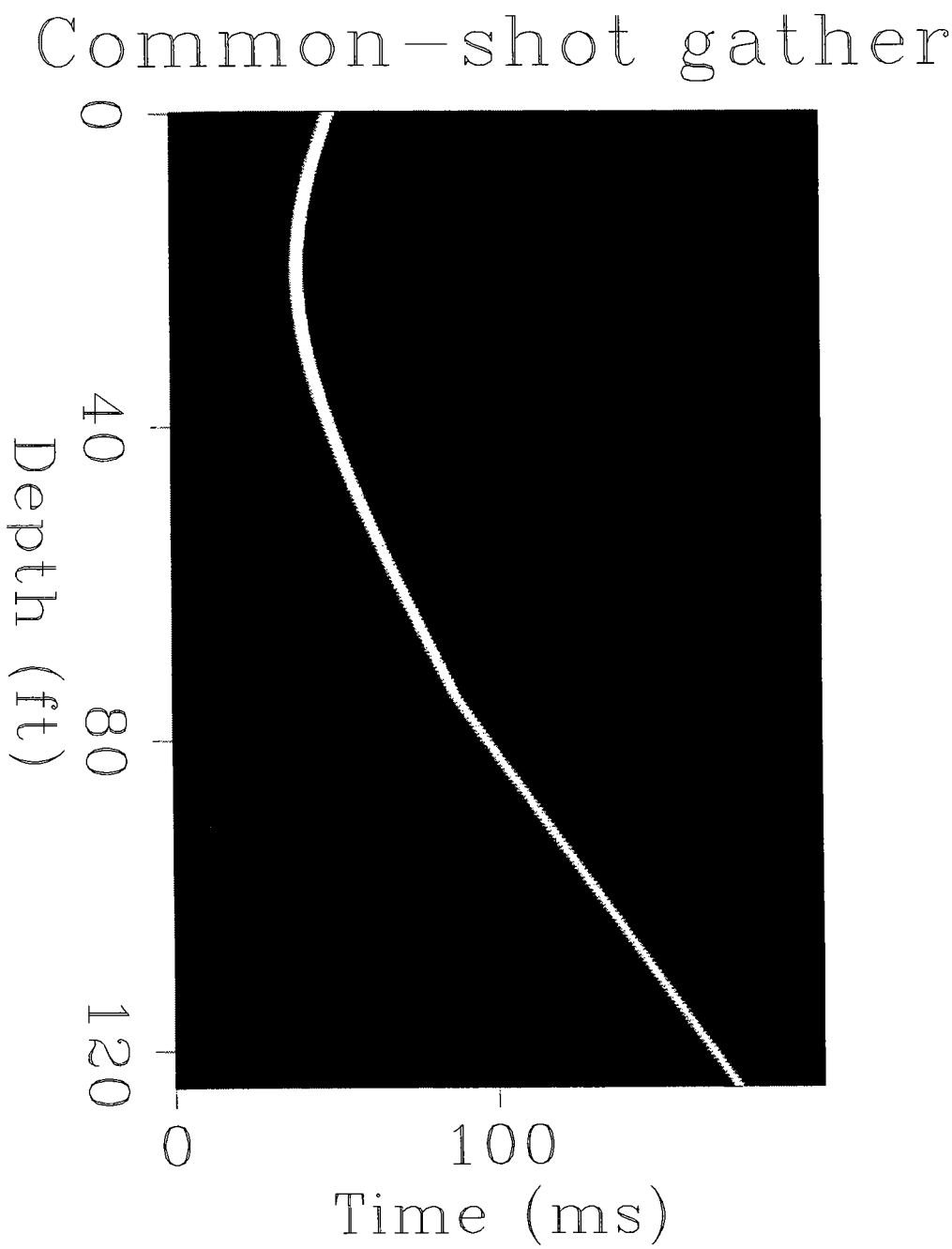

Figure 2. A common shot gather recorded in a 3-D cross-well simulation. The receiver well is off the dip plane from the source. A very good absorbing effect is achieved by an absorbing boundary padding width of 8 grid points, as described in the main text.

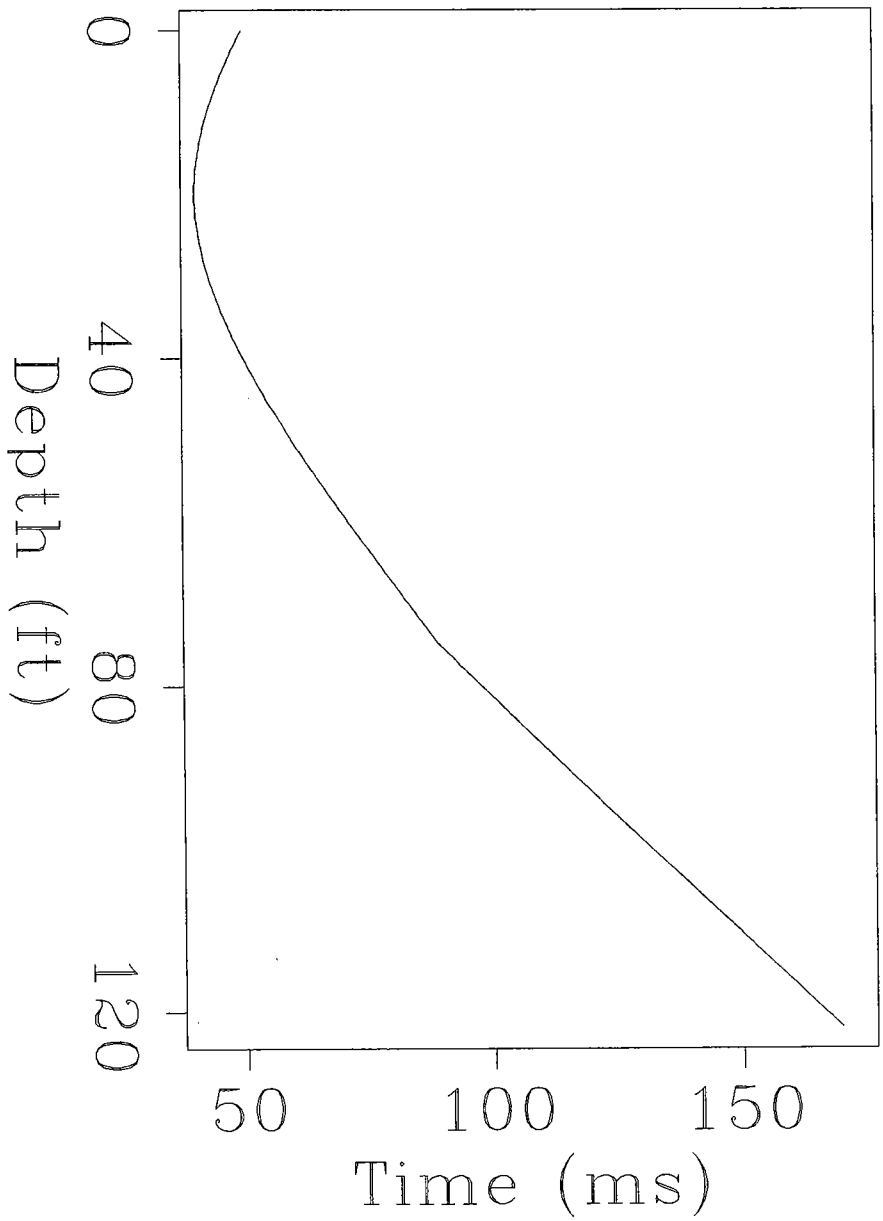

Figure 3. Comparison of the first break travel times of the direct arrival wave forms and the travel times calculated by analytic ray tracing. The match is very good.

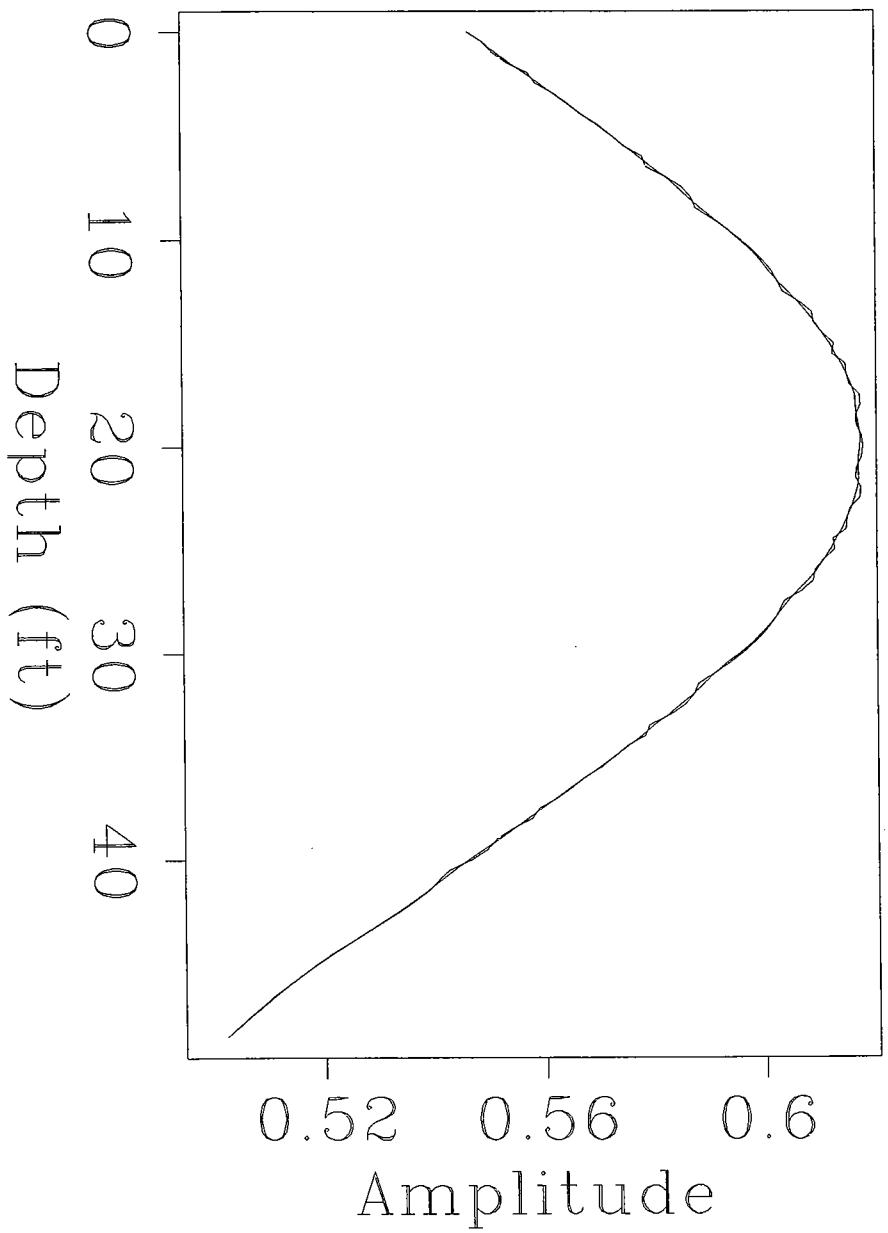

Figure 4. Comparison of the amplitude of the direct arrival wave forms (the jittered curve) and the theoretical 1/r geometrical spreading amplitude (the smooth curve, which is actually a hyperbola).